

**Document Version**

Final published version

**Licence**

CC BY

**Citation (APA)**

Jing, R., Varveri, A., Liu, X., Scarpas, A., & Erkens, S. (2021). Differences in the ageing behavior of asphalt pavements with porous and stone mastic asphalt mixtures. *Transportation Research Record*, 2675(12), 1138-1149. <https://doi.org/10.1177/03611981211032218>

**Important note**

To cite this publication, please use the final published version (if applicable). Please check the document version above.

**Copyright**

In case the licence states "Dutch Copyright Act (Article 25fa)", this publication was made available Green Open Access via the TU Delft Institutional Repository pursuant to Dutch Copyright Act (Article 25fa, the Taverne amendment). This provision does not affect copyright ownership. Unless copyright is transferred by contract or statute, it remains with the copyright holder.

**Sharing and reuse**

Other than for strictly personal use, it is not permitted to download, forward or distribute the text or part of it, without the consent of the author(s) and/or copyright holder(s), unless the work is under an open content license such as Creative Commons.

**Takedown policy**

Please contact us and provide details if you believe this document breaches copyrights. We will remove access to the work immediately and investigate your claim.

## Differences in the Ageing Behavior of Asphalt Pavements with Porous and Stone Mastic Asphalt Mixtures

Transportation Research Record  
2021, Vol. 2675(12) 1138–1149  
© National Academy of Sciences:  
Transportation Research Board 2021



Article reuse guidelines:  
sagepub.com/journals-permissions  
DOI: 10.1177/03611981211032218  
journals.sagepub.com/home/trr



Ruxin Jing<sup>1</sup> , Aikaterini Varveri<sup>1</sup> , Xueyan Liu<sup>1</sup>, Athanasios Scarpas<sup>1,2</sup> , and Sandra Erkens<sup>1</sup>

### Abstract

The degradation of bituminous materials as a result of ageing has a significant effect on asphalt pavement performance. In this study, one porous asphalt (PA) section and one stone mastic asphalt (SMA) asphalt pavement section were designed and constructed in 2014 and exposed to the actual environmental condition. To study the change in the pavement's mechanical properties, asphalt cores were collected from both test sections annually. The change in stiffness modulus was determined via cyclic indirect tensile tests. To investigate the ageing behavior across the pavement depth, the bitumen was extracted and recovered from 13 mm slices along the depths of the cores. The chemical composition and rheological properties of the field-recovered bitumen, and that of original bitumen aged in standard short- and long-term ageing protocols, were investigated by means of the Fourier Transform Infrared (FTIR) spectrometer and Dynamic Shear Rheometer. The results show that the effect of mineral aggregate packing, and therefore of air-void distribution and connectivity, on the ageing sensitivity of the pavements with time was significant, as the changes in the stiffness of the PA mixture were greater than that of SMA mixture. In addition, the results of field-recovered bitumen show that there is an ageing gradient inside the porous asphalt layer, however, the ageing of SMA mainly happens on the surface of the layer. Finally, the field-recovered and laboratory-aged bitumen results demonstrate a weak relation between field and standard laboratory ageing protocols.

Oxidative ageing is one of the most important environmental factors that affect pavement performance and durability (1, 2). During the ageing process, bitumen gradually degrades as a result of oxidative reaction with oxygen in the air, which leads to the hardening and brittleness of the asphalt mixture (3). Eventually, asphalt pavement loses its ability to relax stresses under repeated traffic loading and during the cooling process; thus, the risk of fatigue and cracking damage increases (4, 5).

Pavement ageing includes two stages: short-term ageing (STA), and long-term ageing (LTA) (6). The STA stage mainly occurs during plant mixing, production, transportation, laying down, and compaction (7). In this stage, the effect of ageing is considered to be the same from the surface to the bottom of the asphalt layer, since the temperature and oxygen content are uniform inside the layer. The LTA stage starts after construction. In this stage, the oxygen in the air first reacts with bitumen at the pavement surface. Then, through the connected voids in the asphalt mixture, air flows into the pavement structure and reaches the deeper layers, resulting in ageing along with the pavement depth (8). This process is highly dependent on the

asphalt mixture type (9, 10). Past studies show a clear relationship between the air voids' content and the ageing sensitivity of asphalt mixtures (11). PA mixtures show a higher degree of ageing than dense asphalt mixtures (12). In addition, considering the temperature gradient and the air profile in the pavement structure, LTA is a non-uniform process. Specifically, the pavement surface faces the most severe conditions (13, 14) as it is directly exposed to the atmosphere and suffers the most extreme temperatures (15). Besides, the top layer is exposed to intense sunlight and direct erosion from precipitation. By contrast, the deeper layers below the surface have less contact area with air, a lower temperature gradient, and are affected less by sunlight and moisture (16). As a result, the ageing gradient is formed and developed in the pavement during

<sup>1</sup>Pavement Engineering, Delft University of Technology, Delft, The Netherlands

<sup>2</sup>Civil Infrastructure and Environmental Engineering Department, Khalifa University, Abu Dhabi, United Arab Emirates

**Corresponding Author:**  
Ruxin Jing, r.jing@tudelft.nl

the LTA period and is an important characteristic of field ageing behavior (17–19).

Ageing in the field is quite difficult to investigate as it is a very time-consuming and costly process. To simulate field ageing of bituminous materials in the laboratory, the most commonly used techniques for accelerating ageing are increasing temperature, reducing the materials' thickness, and increasing oxygen concentration by increasing airflow and pressure (20, 21). Existing ageing tests combine these techniques to simulate STA and LTA conditions. The STA and LTA tests used around the world are the rolling thin film oven (RTFO) test and the pressure ageing vessels (PAV) test (22, 23). The RTFO test is considered to represent the bitumen ageing during production and construction, the PAV test is thought to mimic the age hardening of bitumen during the first five to ten years of pavement service life (24). However, more and more results have shown that these laboratory protocols, especially the PAV protocol, cannot describe well the field ageing behavior of pavement (25–28). For example, different mixture types have different ageing sensitivities, and an ageing gradient exists along the pavement depth, which cannot be described by the PAV protocol. Several asphalt mixture laboratory aging protocols have been used recently (29, 30). These procedures can be broadly classified based on the state of the materials during ageing, that is, loose mix and compacted specimens (31, 32). However, the application of these protocols involves challenges related to the slow oxidation rate, the compaction of aged loose mix, and the existence of radial oxidation gradient in the compacted specimen (33–35), and so forth.

Therefore, field data from different types of asphalt mixtures under diverse climatic conditions are necessary and important to better understand the field ageing behavior of pavement and to further develop a proper laboratory ageing protocol.

## Objectives

This work focuses on evaluating the difference in the ageing behavior of porous asphalt (PA) and stone mastic asphalt (SMA) pavements. To achieve this, the three objectives of this study were to: i) investigate the effect of field ageing on the PA and SMA mixture; ii) determine the changes in the chemical composition and mechanical properties of field-recovered bitumen from different depths; and iii) compare the chemical and stiffness results of field-recovered bitumen with standard laboratory-aged bitumen.

## Materials and Methods

### Materials and Mixture Design

PA and SMA mixtures are commonly used on national highways and provincial roads in the Netherlands. In this

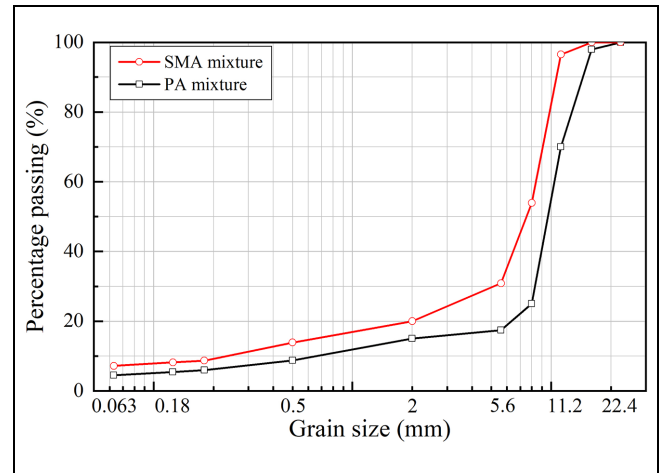


**Figure 1.** Gradations of PA and SMA mixtures.

Note = SMA = stone mastic asphalt; PA = porous asphalt.

study, one PA and one SMA mixture were designed using the aggregate gradations shown in Figure 1. The same type of PEN 70/100 bitumen, one of the most commonly used in the Netherlands, was used for both mixtures. The bitumen content was 5.0% and 6.4% based on the total weight of mix for the PA and the SMA mixtures, respectively. A factory limestone filler with 26.4% calcium hydroxide, that is, Wigro 60K filler, was used for both mixtures. Wigro 60K is the commonly used filler in the Netherlands because of its contribution to improving the moisture sensitivity of pavements (36–38). For both mixtures, crushed sandstone, that is, Norwegian sandstone was used, with a nominal maximum size of 16 mm. The target air-void content was 16% and 5% for the PA and SMA mixtures, respectively. The SMA is referred to as dense mixture. This term does not describe the mix type (e.g., open-graded, dense-graded, gap-graded, etc.) but refers to the low void content of the SMA mix compared with the PA mix, which has a high void content. Table 1 summarizes the specifications of the materials studied, that is, bitumen, filler, and aggregate.

### Tests on Asphalt Pavement Cores

In this study, samples with a diameter of 100 mm and a thickness of 50 mm were cored from the PA and SMA test sections every year since 2014. The details of the construction of the test sections can be found in previous reports (26, 39, 40). The dynamic modulus (stiffness) of asphalt mixtures can be used in the Mechanistic-Empirical Pavement Design Guide (MEPDG) to determine pavement thickness and predict pavement performance. Considering its thickness and diameter, the dynamic modulus of the core was determined by means of the Cyclic Indirect Tensile Test (IT-CY) according to NEN-EN 12697-26. For each mixture, three replicates were tested using the Universal Testing Machine (UTM) at five

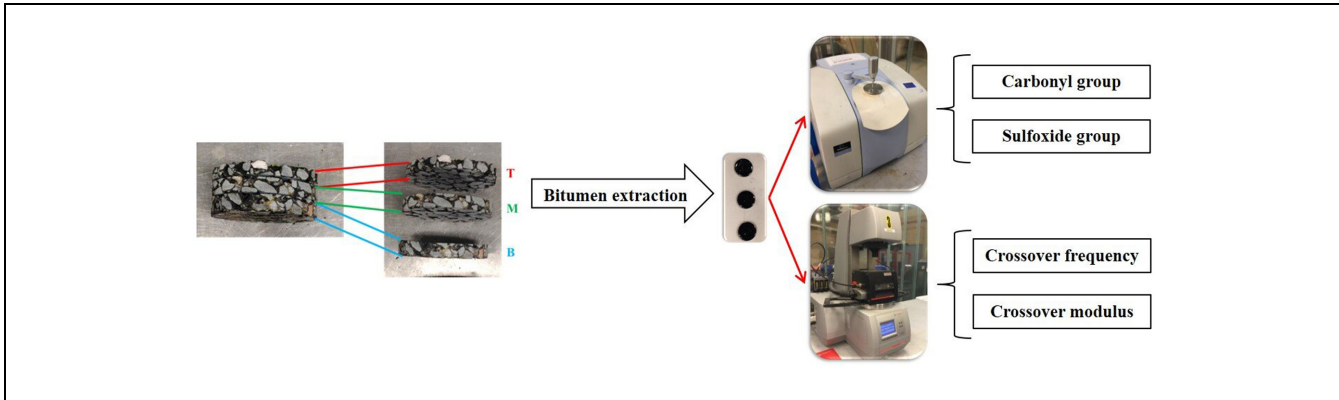


**Figure 2.** Tests performed on field-recovered bitumen.

**Table 1.** Specification of Materials Studied

Properties	Unit	Value
PEN 70/100 bitumen (from Q8 oils)		
Penetration at 25°C	0.1 mm	70–100
Softening point	°C	43–51
Dynamic viscosity at 60°C	Pa s	160
Complex shear modulus at 1.6 Hz and 60°C	kPa	1.8
Phase angle at 1.6 Hz and 60°C	°	88
Wigro 60K filler		
Bitumen number	ml/100 g	59
Ca(OH) <sub>2</sub> content	%	26.4
Mass loss at 110°C	%	0.4
Water solubility	%	6.1
Density	kg/m <sup>3</sup>	2,780
Fractional voids (Ridgen)	%	47
Norwegian sandstone		
Density	kg/m <sup>3</sup>	2,740
Uniaxial compressive strength	MPa	150
Tensile strength	MPa	15
Young's modulus	GPa	30
Poisson's ratio		0.20

frequencies, that is, 0.5, 1, 2, 5, and 10 Hz and four testing temperatures that is, 0°C, 10°C, 20°C, and 30°C. The conditioning time before testing was set to 4 h to balance the temperature of the sample. The effect of time/frequency and temperature on the mechanical behavior of the viscoelastic asphalt materials was described by master curves using the time-temperature superposition (TTS) principle. The results of the IT-CY test offer a better understanding of the evolution of mixture stiffness.

### Tests on Field-Recovered Bitumen

To compare the effect of ageing at different depths, the PA and SMA cores from 2018 (recently collected samples from the field) were cut into three 13-mm slices from top to bottom, and the remaining part was discarded. The slices are marked with T (Top), M (Middle), and B

(Bottom), (Figure 2). Bitumen was extracted from the slices by using the fully automatic bitumen extraction apparatus according to the EN 12697-1 European standard. Dichloromethane was used as a solvent during bitumen extraction. Vacuum evaporation using a rotary evaporator was conducted to separate the solvent from bitumen. After the recovery of bitumen, Fourier Transform Infrared (FTIR) tests were performed to check if the solvent was fully evaporated. If the solvent was still present in the sample, this would appear in the FTIR results as two special peaks (at around 1,250 cm<sup>-1</sup> and 750 cm<sup>-1</sup>) in the spectrum (26).

FTIR spectroscopy is generally adopted as a tool to monitor the changes in the chemical composition of bitumen after ageing and to quantify oxidation. In this study, a Perkin Elmer Spectrum 100 FTIR spectrometer was used in the attenuated total reflectance (ATR) mode to identify the chemical functional groups of the bitumen. The sample was scanned 20 times with a fixed instrument resolution of 4 cm<sup>-1</sup>. The wavenumbers range was set to vary from 600 to 4,000 cm<sup>-1</sup>. At least three repetition tests were done for each ageing condition.

The rheological properties of field-recovered bitumen were characterized by means of Dynamic Shear Rheometer (DSR) according to NEN-EN 14770. The bitumen samples were tested using the parallel-plates configuration. Initially, the linear viscoelastic (LVE) strain range of bitumen samples was determined using amplitude sweep tests. The frequency sweep tests were performed at five different temperatures (0°C, 10°C, 20°C, 30°C, and 40°C). During the tests, the frequency varied in a logarithmic manner from 50 Hz to 0.01 Hz. At least three repetition tests were done for each ageing condition.

For comparison, the virgin PEN 70/100 bitumen was subjected to standard laboratory ageing. To be specific, STA was simulated by using the RTFO test at 163°C for 75 min, in accordance with the EN 12607-1 test standard. LTA was simulated by using PAV at 100°C and 2.1 MPa

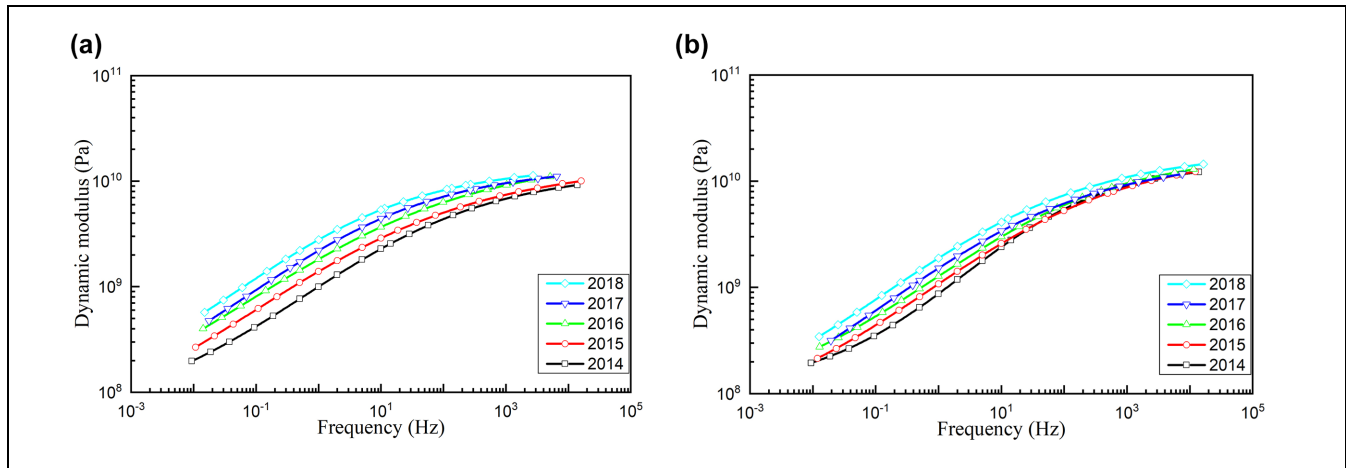


**Figure 3.** Master curve of asphalt mixture at reference temperature 20°C: (a) PA mixture; (b) SMA mixture.

Note: PA = porous asphalt; SMA = stone mastic asphalt.

(20 atm) for 20 h, according to the EN 14769 ageing standard. Then the chemical and rheological properties of bitumen at fresh, STA, and LTA conditions were also evaluated using FTIR and DSR.

To better understand the ageing effect at various pavement depths, the low temperature and fatigue properties of field-recovered bitumen were evaluated by means of relaxation and linear amplitude sweep (LAS) tests. Since ageing normally has a positive effect on high temperature properties as a result of material hardening, the high temperature tests, such as the multiple stress creep and recovery (MSCR) test, were not performed in this study. The relaxation tests were performed with 1% shear strain in a very short time period (0.1 s) at the beginning, followed by a relaxation period of 100 s. The bitumen samples were tested using the parallel-plates configuration with 8 mm plate diameter and 2 mm gap at 0°C. The shear stress values were collected during the tests. Since the relaxation rate is very fast at the beginning of the test, the data is collected every 0.01 s. The LAS tests are intended to evaluate the ability of bitumen materials to resist damage by employing cyclic loading at increasing amplitudes to damage. The shear strain varied linearly from 0% to 30% and data were recorded per second. The bitumen samples were tested using the parallel-plates configuration with 8 mm plate diameter and 2 mm gap at 20°C. The characteristics of the damage accumulation rate in the material were used to indicate the fatigue behavior of bitumen.

## Results and Discussion

### Mixture Stiffness

According to the TTS principle, the master curve of the dynamic modulus was generated at a reference temperature of 20°C. Figure 3 shows the evolution of stiffness for the PA and SMA mixtures from 2014 to 2018.

Overall, the dynamic modulus of both PA and SMA mixtures increases with time. The rate of modulus change is higher for the PA than for the SMA mixture. This is mainly because of the high void content of PA, which leads to inherently high sensitivity to oxidative ageing. According to the CT scan results of core samples, the PA mixture had 16% and the SMA mixture had 5% of air voids, as shown in Figure 4. It has been found that the high air-void content of PA results in high interconnectivity of the voids network, in which more than 90% of the total air voids are interconnected, while less than 10% of the total air voids have been reported to be interconnected in SMA mixtures (41).

More interestingly, from Figure 3 it can be observed that the change in the dynamic modulus for both mixtures is significantly higher for two periods, namely from 2015 to 2016 and from 2017 to 2018. The weather data that were collected from the weather station close to the test sections show the fluctuations in the yearly mean temperature and the number of days with high temperatures (more than 10°C) over the years from 2015 to 2018. Figure 5a shows that the yearly mean temperature in 2016 and 2018 was about 1°C higher than in 2015 and 2017. Also, Figure 5b demonstrates that daily mean temperature exceeded 10°C for 217 days in 2016 and 215 days in 2018, while 200 and 186 days were recorded in 2015 and 2017. Overall, the years 2016 and 2018 were in general warmer than 2015 and 2017. Additionally, the yearly change in stiffness of two mixtures at 20°C and 10 Hz were added in Figure 5. It can be observed that there is a strong correlation between climatic conditions and the stiffness changes.

### Changes in the Chemical Functionality of Bitumen

The FTIR tests were performed on fresh, laboratory-aged and field-recovered bitumen samples (from the different

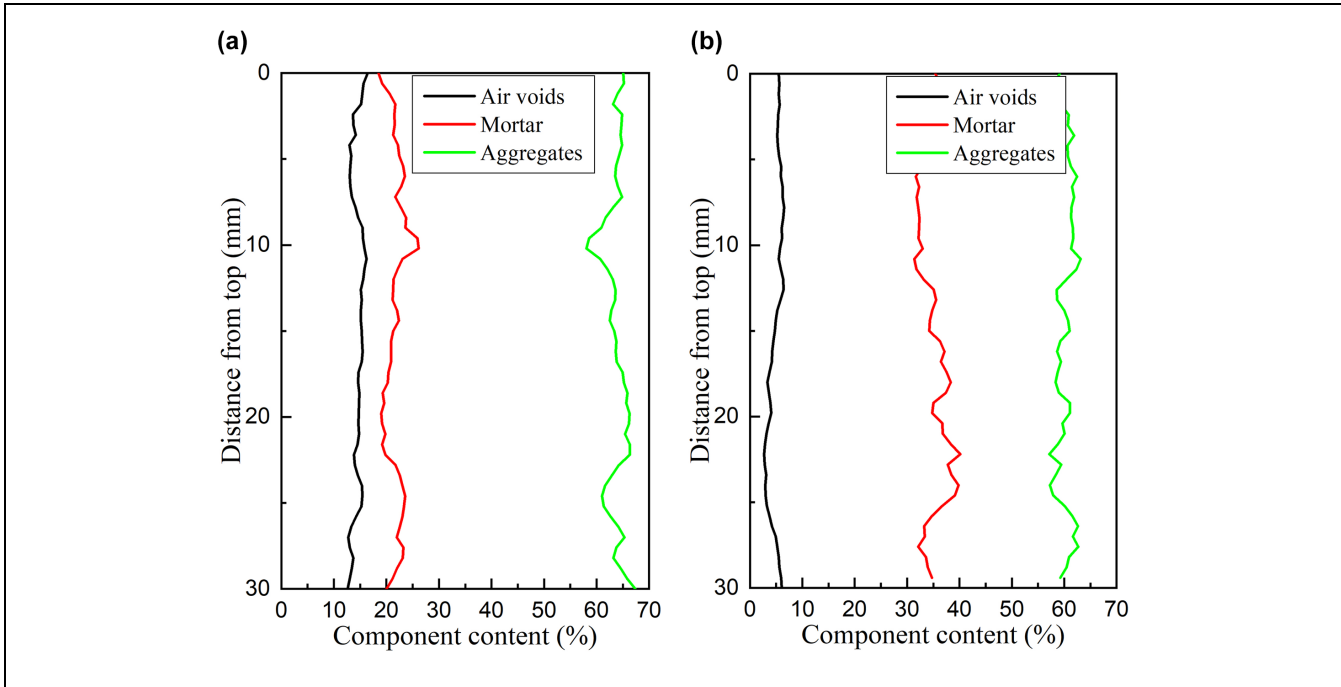


**Figure 4.** Distribution of air voids, mortar and aggregates over the height of the core sample: (a) PA mixture; (b) SMA mixture (42). Note: PA = porous asphalt; SMA = stone mastic asphalt.

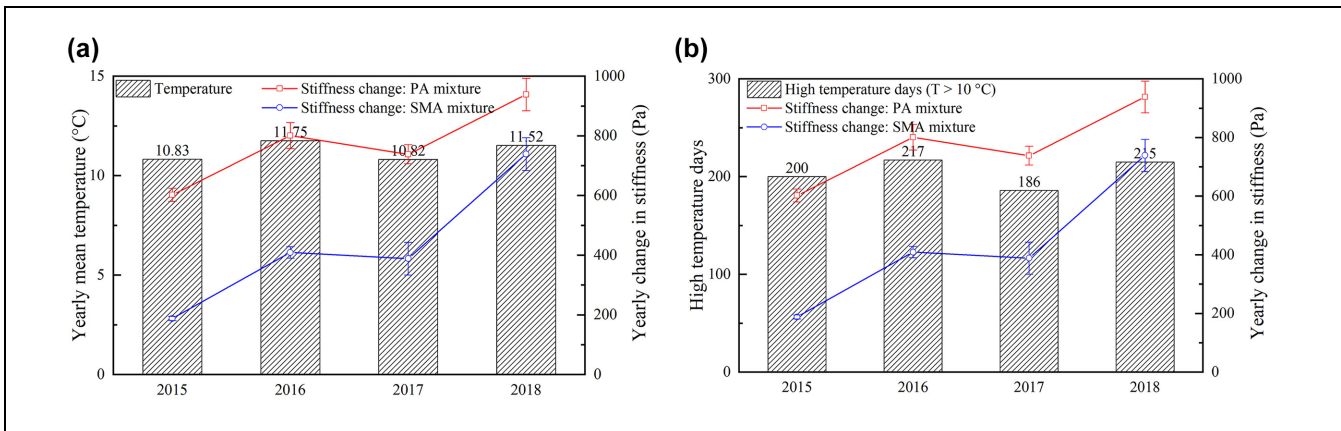


**Figure 5.** Temperature information from 2015 to 2018: (a) yearly mean temperature; (b) high temperature days. Note: PA = porous asphalt; SMA = stone mastic asphalt.

slices of the 2018 core samples) to determine their chemical changes as a result of ageing. The carbonyls group (C=O) at 1,753 to 1,660  $\text{cm}^{-1}$  wavenumbers and the sulfoxides group (S=O) band at 1,047 to 995  $\text{cm}^{-1}$  wavenumbers, in the FTIR spectrum, were used to quantify bitumen oxidation. The carbonyl and sulfoxide indices were calculated using Equations 1 and 2 to quantify the changes in the area under the two peaks using the vertical limit bands as shown in Figure 6 (26, 30, 43).

$$\text{Carbonyl index} = \frac{A_{1700}}{\sum A} \quad (1)$$

$$\text{Sulfoxide index} = \frac{A_{1030}}{\sum A} \quad (2)$$

where  $\sum A = A_{(2953,2923,2862)} + A_{1700} + A_{1600} + A_{1460} + A_{1376} + A_{1030} + A_{864} + A_{814} + A_{743} + A_{724}$

The quantitative indices for carbonyls and sulfoxides of laboratory-aged and field-recovered bitumen are shown in Figure 7. Overall, the results show that the formation of carbonyls and sulfoxides were higher for the bitumen samples recovered from the PA than those from SMA. These results suggest that PA has a higher ageing sensitivity than SMA, which agrees with the stiffness

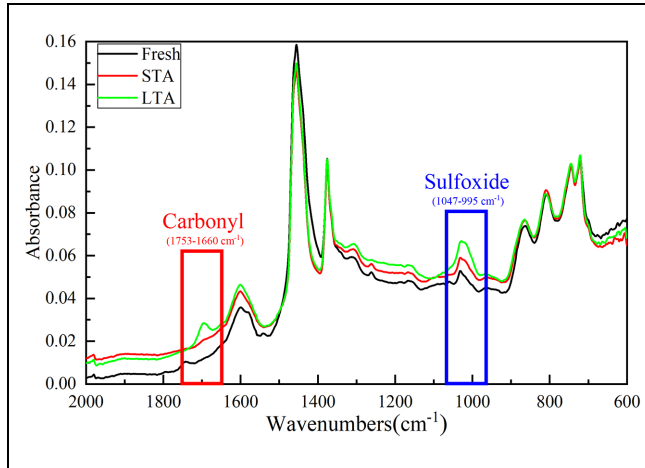


**Figure 6.** FTIR spectra of laboratory-aged bitumen.  
Note: STA = short-term ageing; LTA = long-term ageing.

results of the core samples presented in the previous section.

Moreover, the ageing indices across the pavement depth are significantly different between PA and SMA mixtures. For both mixture types, ageing at the top slice

(pavement surface) is more severe as indicated by the higher values of the ageing indices in comparison to those at lower pavement depths as a result of the direct exposure to the atmospheric oxygen and temperature. For the PA mixture, it can be observed that the ageing index gradually decreases from top to bottom. However, for the SMA mixture, the top slice has the highest ageing index compared with the middle and bottom slices, which have similar values but significantly lower values than at the top. These findings suggest that ageing has a full-depth effect on PA pavements, but its impact on SMA pavement mainly occurs at the surface.

To identify the difference in the chemical ageing indices of PA and SMA, as a further step, the values of the carbonyl and sulfoxide indices are presented in Table 2. In addition, a t-test was performed to evaluate any statistical difference. A 95% confidence level was selected, and the statistical analysis results are shown in Table 2. As can be seen from the table, there is no significant difference in the ageing indices of PA and SMA considering the results of the top slice. However, the difference in the ageing indices of PA and SMA at the middle and bottom are shown to be statistically significant.

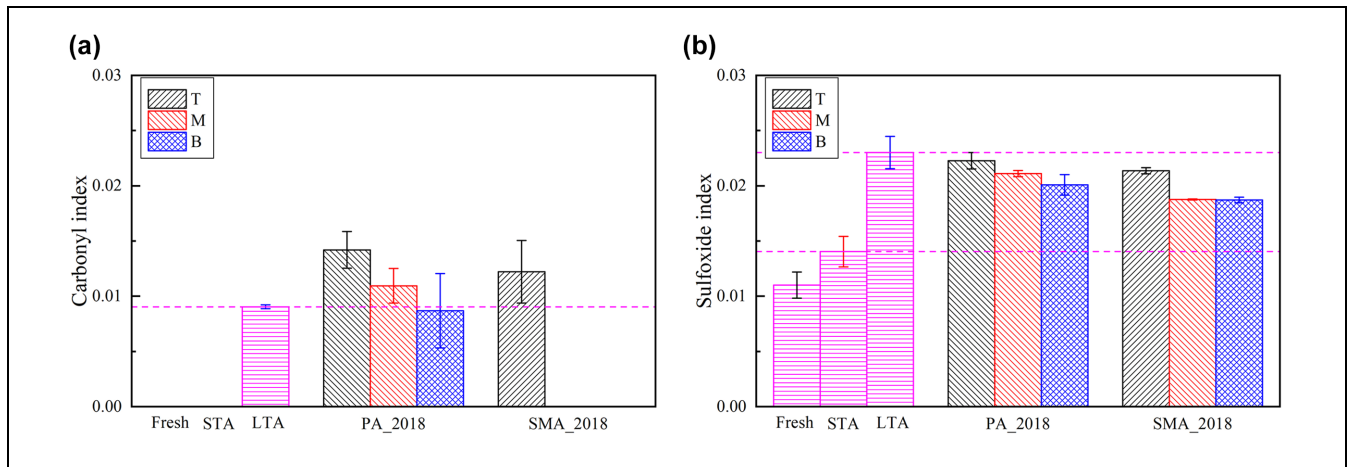


**Figure 7.** Ageing indices of laboratory-aged and field-recovered bitumen: (a) carbonyl index; (b) sulfoxide index.  
Note: PA = porous asphalt; SMA = stone mastic asphalt; STA = short-term ageing; LTA = long-term ageing.

**Table 2.** Quantitative and Statistical Analysis of Carbonyl and Sulfoxide Indices of PA and SMA

Ageing index	Slice	PA_2018	SMA_2018	P-value	Significantly difference (at 95% confidence level)
Carbonyl index	T	0.0142	0.0122	0.27	No
	M	0.0110	0	<0.01	Yes
	B	0.0087	0	<0.01	Yes
Sulfoxide index	T	0.0223	0.0214	0.06	No
	M	0.0211	0.0188	<0.01	Yes
	B	0.0201	0.0187	0.03	Yes

Note: PA = porous asphalt; SMA = stone mastic asphalt.

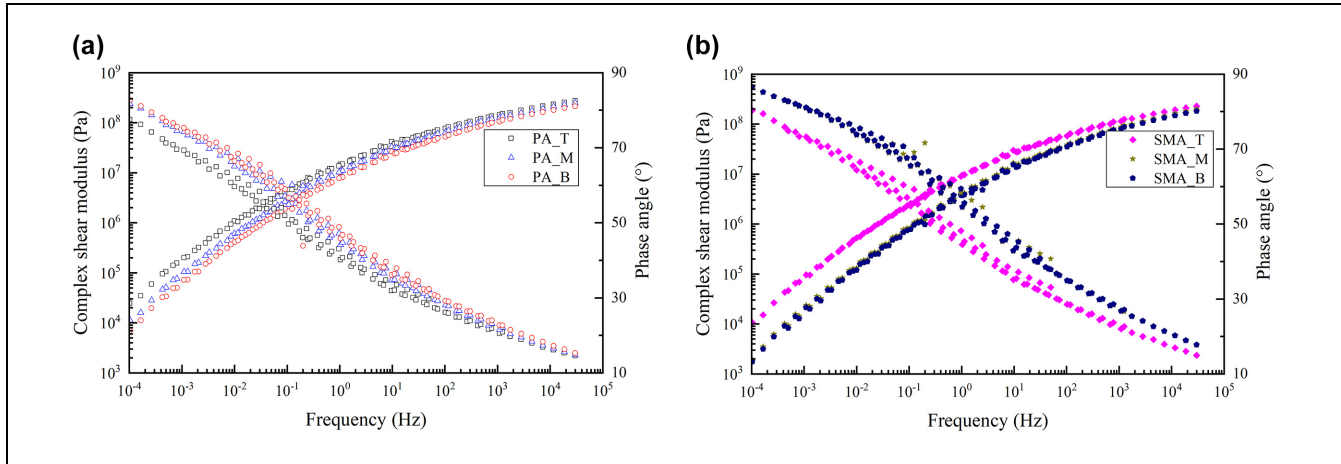


**Figure 8.** Master curves of complex shear modulus and phase angle of field-recovered bitumen of: (a) PA mixture; (b) SMA mixture. STA = short-term ageing; LTA = long-term ageing.

To be specific, the carbonyl index of PA is 0.0110 and 0.0087 at the middle and bottom slices, respectively, while no carbonyl functional groups were detected at the middle and bottom slices of SMA. The sulfoxide index of PA is 0.0211 and 0.0201 at the middle and bottom slices respectively, which is about 10% higher than that of SMA at the corresponding slices.

From a comparison between the results of laboratory-aged and field-recovered bitumen for both the PA and SMA mixtures, the carbonyl index of the recovered bitumen is higher than that of LTA. This can be explained by the different conditions that are present during laboratory and field ageing. For instance, laboratory ageing is performed at relatively high temperatures (100°C in this study), while field ageing of pavement occurs at lower temperature and is accompanied by moisture and UV effects. On the other hand, the sulfoxide index of the recovered bitumen is smaller than that of LTA. This may also be caused by the combined ageing-moisture effects. According to some studies, the sulfoxides are water soluble and can be removed by water in the field condition (44–46).

### Change in the Rheological Properties of Bitumen

To compare the effect of ageing at different depths, the rheological properties of recovered bitumen from the PA and SMA cores of 2018 were studied. The viscoelastic behavior of bitumen in a wide range of frequencies was described using the master curves of complex shear modulus and phase angle at a reference temperature 20°C on the basis of the TTS principle. As expected, the complex shear modulus increases and the phase angle decreases with ageing. Figure 8 shows that PA and SMA mixtures have higher complex shear modulus and lower phase angle at the top slice compared with the middle and bottom slices. As expected, such results indicate that ageing

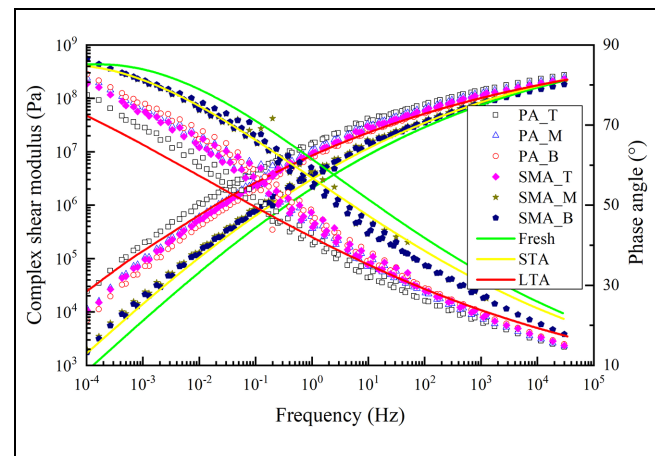


**Figure 9.** Comparison of master curves (complex shear modulus and phase angle) of laboratory-aged and field-recovered bitumen. Note: PA = porous asphalt; SMA = stone mastic asphalt; STA = short-term ageing; LTA = long-term ageing.

is more severe for the top part of the pavement. In addition, for the PA mixture (Figure 8a), it can be observed that the complex shear modulus decreases and the phase angle increases from the top to the bottom slices. While, for SMA mixture (Figure 8b), the middle and bottom slices have consistent complex shear modulus and phase angle values across the frequency spectrum. These results point out that ageing affects the PA mixture throughout its depth, whereas for SMA mixture the ageing effects are mainly found on the surface. This observation agrees well with the chemical profiles of the PA and SMA mixtures as discussed in the previous section.

For comparison, the master curves of complex shear modulus and phase angle of laboratory-aged and field-recovered bitumen are illustrated in Figure 9. The results show that PA has a higher complex shear modulus and

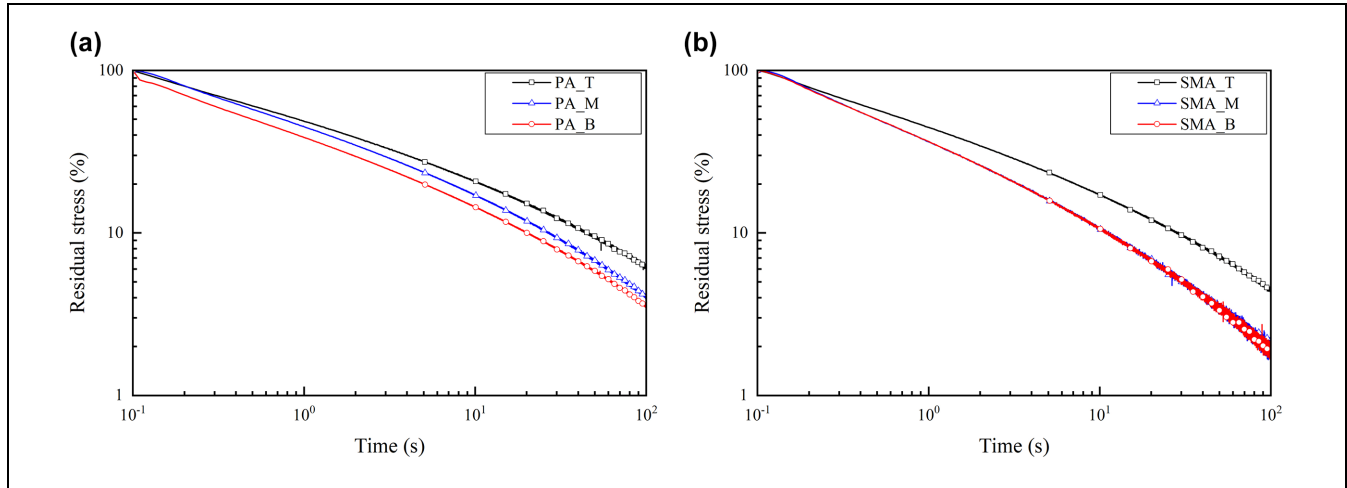


**Figure 10.** Relaxation curves of field-recovered bitumen: (a) PA mixture; (b) SMA mixture. Note: PA = porous asphalt; SMA = stone mastic asphalt.

lower phase angle than SMA at the corresponding slices. As expected, it suggests that PA has a higher ageing rate because of its high porosity. In addition, the master curves show that the stiffness of the bitumen recovered from the top slice (PA\_T) is higher than that of LTA sample, whereas the top slice of SMA (SMA\_T) has approximately the same stiffness as the LTA sample. It appears that the ageing state of the top slices of the PA and SMA is more severe than or similar to the LTA sample. These results imply again that the long-term field ageing condition cannot be simulated accurately by the PAV protocol. Moreover, the middle and bottom slices of the SMA (SMA\_M and SMA\_B) have slightly higher stiffness and lower phase than the STA samples. This means that the SMA mixture has a better ageing resistance because of its high density that prevents oxygen flow into the pavement structure and slows down ageing inside the pavement structure.

To better distinguish the ageing behavior across the PA and SMA pavement depths, the relaxation and fatigue properties were evaluated by means of relaxation and LAS tests. As in the frequency sweep tests, a minimum of three replicate samples for each condition were tested.

By normalizing the initial shear stress to a value of 100%, the residual stress versus relaxation time of the field-recovered bitumen is plotted in Figure 10 and shows that a power law can describe well the relationship between the residual stress and relaxation time. For both mixtures, the relaxation curve of the top slice (PA\_T, SMA\_T) is above that of the middle and bottom slices (PA\_M, PA\_B, SMA\_M, SMA\_B), indicating that at the same relaxation time the residual stress after unloading is higher at top slice than the other two slices. The differences in the relaxation properties with pavement depth would lead to stress concentrations at the pavement

surface. The repeated traffic loading can cause an accumulation of stresses and fatigue in the mortar bridges that hold the coarse aggregates together, which can further lead to raveling. Similar to the chemical and stiffness results, the relaxation properties show a gradient with pavement depth for the PA, whereas for the SMA they are more pronounced at the surface.

To further quantify the relaxation properties of field-recovered bitumen, two relaxation indices, explicitly the residual stress at 100 s and the relaxation time at which shear stress reduces to 25% of the initial, were evaluated and are presented in Figure 11 (47). The results show that the residual stress and relaxation time decrease from top to bottom slices. Comparing the results of the two mixtures, it can be observed that higher residual stresses exist and longer relaxation time is needed for the PA mixture than for the SMA mixture at the corresponding depths.

According to the AASHTO Designation TP 101-14 (48, 49), the fatigue analysis was performed on the LAS results. Then based on the viscoelastic continuum damage (VECD) theory (50), the fatigue life of bitumen can be fitted using Equation 3.

$$N_f = A\gamma^{-B} \tag{3}$$

where,

$N_f$  is the number of cycles to failure,

$\gamma$  is the shear strain and, and

$A$  and  $B$  are fitting parameters derived from the experiment.

The fatigue results of the field-recovered bitumen are obtained and fitted according to Equation 3, and plotted in Figure 12. The fitting parameters,  $A$  and  $B$ , are reported in Figure 13.

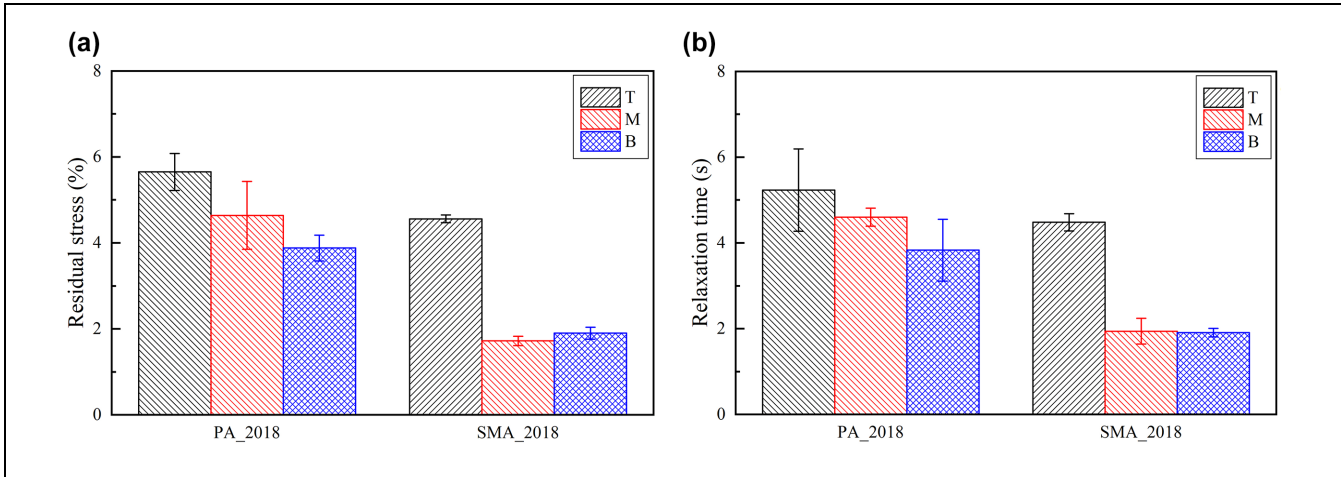


**Figure 11.** Relaxation indices of recovered bitumen: (a) residual stress at 100 s; (b) relaxation time at the shear stress levels of 25% of the initial stress.  
 Note: PA = porous asphalt; SMA = stone mastic asphalt.

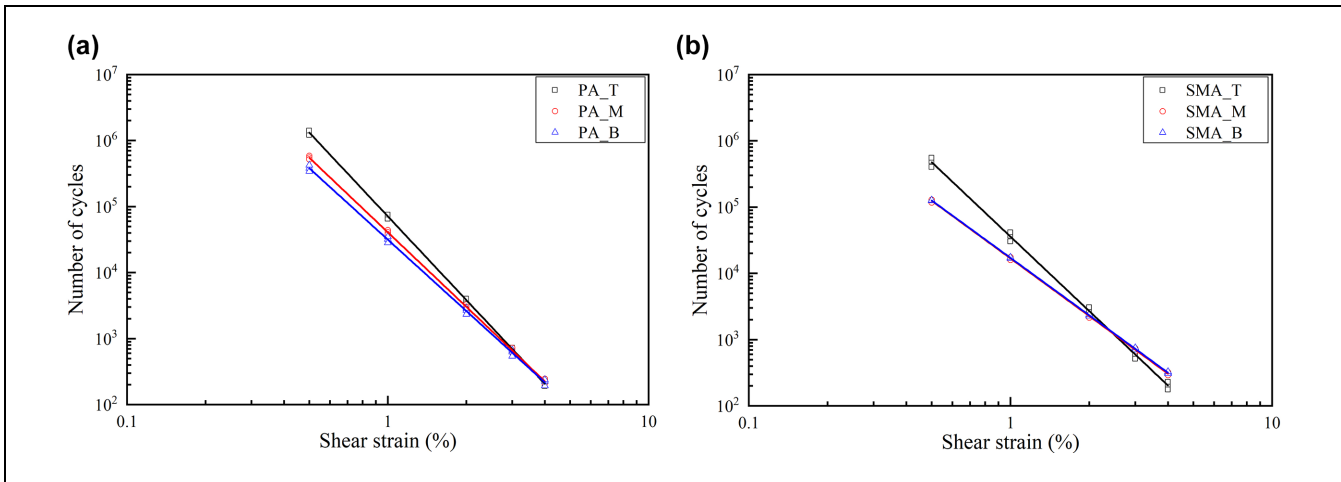


**Figure 12.** Fatigue results of field-recovered bitumen: (a) PA mixture; (b) SMA mixture.  
 Note: PA = porous asphalt; SMA = stone mastic asphalt.

Overall, the rotation of the fatigue curve is more pronounced for the top slice compared with the bottom slices, as shown in Figure 12, suggesting that the fatigue life of the top part of the pavement increases under low loading levels and decreases under high loading levels. This finding indicates that, as bitumen becomes stiffer and more brittle because of ageing, it can undertake more loading cycles under low loading levels; by contrast, it can sustain less loading cycles under high loading levels because of its increased brittleness. Comparing the fitting parameters of the two mixtures, Figure 13, PA has higher values of the parameters A and B than SMA at the corresponding depths. This means that the change in fatigue life of PA is higher than that of SMA because of severe ageing as a result of its high porosity. In

addition, the profile of the fatigue property with the pavement depths are consistent with the chemical, stiffness, and relaxation results. The differences in the fatigue properties with pavement depth may indicate the position where the fatigue damage occurs and the direction of the fatigue crack propagation (51, 52).

### Conclusions and Recommendations

Identifying the ageing behavior of various asphalt mixtures in the field is important for the development of artificial laboratory ageing protocols that allow for reliable predictions of long-term performance of asphalt pavements. For this reason, asphalt pavement sections with one PA and one SMA test section were constructed in

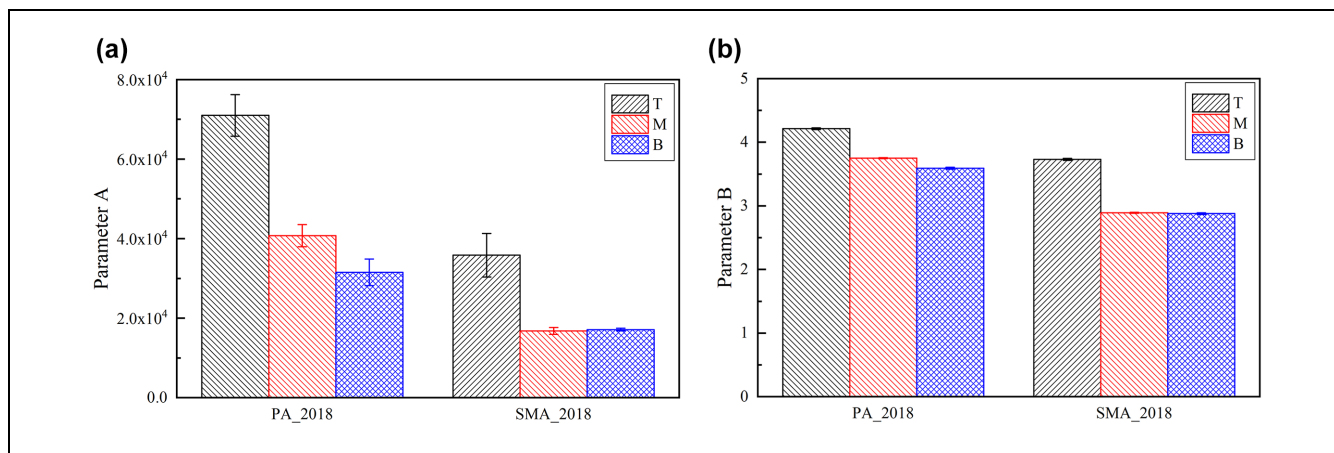


**Figure 13.** Fitting parameters of fatigue results: (a) parameter A; (b) parameter B. Note: PA = porous asphalt; SMA = stone mastic asphalt.

2014 and continuously exposed to environmental conditions.

The results show that field ageing has more influence on PA mixtures than on SMA mixtures, because of the high void content of the PA mixtures, which leads to a larger binder area directly exposed to oxygen and temperature. The chemical and rheological results of the field-recovered bitumen show that oxidative ageing is more severe at the pavement surface. In addition, a significant difference in the field ageing behavior of the PA and SMA mixtures is observed along the pavement depth. Specifically, an ageing gradient exists in the PA mixture, whereas the ageing of the SMA mixture mainly occurs at the surface. This can be explained by the high porosity, and therefore by the highly interconnected air voids network in the PA, which allows oxygen to easily penetrate into the asphalt layer; by contrast, the SMA mixture has low interconnectivity that slows down the oxidative ageing in the deeper layers. Finally, the comparison between the field-recovered and the laboratory-aged results demonstrate that there is a weak relationship between field ageing and the standard ageing protocols. Four years of field ageing at the pavement surface is far more severe than the ageing caused by standard laboratory ageing protocols. Moreover, the PAV protocol does not consider the ageing sensitivity of various mixtures and cannot reflect the ageing gradient along the pavement depth.

As a continuation of this research, an experimental testing program is currently being undertaken on the asphalt mixture and extracted bitumen with the aim of developing a proper ageing protocol to simulate the long-term and field ageing behavior of PA and SMA mixtures. In addition, the rheological and chemical profiles of field-recovered bitumen result from the synergistic effects of thermal-oxidative ageing, photo-oxidative (ultraviolet radiation), and moisture. To fully characterize the field

ageing behavior of asphalt pavement, the various environmental factors need to be coupled in the laboratory protocols.

### Acknowledgments

The authors gratefully acknowledge the Dutch Ministry of Transport, Public Works and Water Management for funding this project.

### Author Contributions

Planning and supervision of the construction of the test sections: R. Jing and X. Liu; experimental plan and interpretation of the results: R. Jing and A. Varveri; experiments: R. Jing; supervision of project activities: A. Scarpas and S. Erkens. All authors were involved in evaluating the results and contributed to the final manuscript.




### Declaration of Conflicting Interests

The author(s) declared no potential conflicts of interest with respect to the research, authorship, and/or publication of this article.

### Funding

The author(s) received no financial support for the research, authorship, and/or publication of this article.

### ORCID iDs

Ruxin Jing  <https://orcid.org/0000-0001-6975-807X>  
 Aikaterini Varveri  <https://orcid.org/0000-0002-8830-9437>  
 Athanasios Scarpas  <https://orcid.org/0000-0002-3478-8807>

### References

1. Isacson, U., and H. Zeng. Relationships between Bitumen Chemistry and Low Temperature Behavior of Asphalt.

- Construction and Building Materials*, Vol. 11, No. 2, 1997, pp. 83–91.
2. Petersen, J. C., and R. Glaser. Asphalt Oxidation Mechanisms and the Role of Oxidation Products on Age Hardening Revisited. *Road Materials and Pavement Design*, Vol. 12, No. 4, 2011, pp. 795–819.
  3. Chai, G., R. van Staden, S. H. Chowdhury, and Y. C. Loo. A Study of the Effects of Pavement Ageing on Binder Deterioration. *International Journal of Pavement Engineering*, Vol. 15, No. 1, 2014, pp. 1–8.
  4. McGovern, M. E., W. G. Buttlar, and H. Reis. Field Assessment of Oxidative Ageing in Asphalt Concrete Pavements with Unknown Acoustic Properties. *Construction and Building Materials*, Vol. 116, 2016, pp. 159–168.
  5. Woo, W., A. Chowdhury, and C. Glover. Field Ageing of Unmodified Asphalt Binder in Three Texas Long-Term Performance Pavements. *Transportation Research Record: Journal of the Transportation Research Board*, 2008. 2051(1): 15–22.
  6. Mirza, M. W., and M. W. Witzak. Development of a Global Ageing System for Short and Long Term Ageing of Asphalt Cements. *Journal of Association of Asphalt Pavement*, Vol. 64, 1995, pp. 393–430.
  7. Petersen, J. C. Accelerated Ageing Test for Evaluating Asphalt Oxidative Ageing. *Association of Asphalt Paving Technologists Proceedings*, Vol. 58, 1989, pp. 220–237.
  8. Lee, D. Y. *Development of a Durability Test for Asphalts*. Iowa Highway Research Board Project HR-124, Final Report ISU-ERI-72125. Engineering Research Institute, Iowa State University, 1972.
  9. Erkens, S., L. Porot, R. Glaser, and J. Glover. Ageing of Bitumen and Asphalt Concrete: Comparing State of the Practice and Ongoing Development in the United States and Europe. Presented at 95th Annual Meeting of the Transportation Research Board, Washington, D.C., 2016.
  10. Huang, S., and M. Zeng. Characterization of Ageing Effect on Rheological Properties of Asphalt-Filler System. *International Journal of Pavement Engineering*, Vol. 8, No. 3, 2007, pp. 213–223.
  11. Lu, X., P. Redelius, H. Soenen, and M. Thau. Material Characteristics of Long Lasting Asphalt Pavement. *Road Materials and Pavement Design*, Vol. 12, No. 3, 2011, pp. 567–585.
  12. Jemere, Y. Development of a Laboratory Ageing Method for Bitumen in Porous Asphalt. Masters thesis. Delft University of Technology, 2010.
  13. Al-Khateeb, G., X. Qi, A. Shenoy, K. Stuart, and T. Mitchell. Assessment of Ageing at FHWA's Pavement Testing Facility. *Transportation Research Record: Journal of the Transportation Research Board*, 2005. 1940: 146–155.
  14. Klierer, J. E., H. Zeng, and T. S. Vinson. Ageing and Low-Temperature Cracking of Asphalt Concrete Mixture. *Journal of Cold Region Engineering*, Vol. 10, No. 3, 1996, pp. 134–148.
  15. Sen, S., and J. Roesler. Ageing Albedo Model for Asphalt Pavement Surfaces. *Journal of Cleaner Production*, Vol. 117, 2016, pp. 167–175.
  16. Glover, C. J., R. R. Davison, C. H. Domke, Y. Ruan, P. Juristyarini, and D. B. Knorr. *Development of a New Method for Assessing Asphalt Binder Durability with Field Validation*. Report FHWA/TX-03/1872-2. Texas Transportation Institute College Station, 2005.
  17. Kim, Y. R., C. Castorena, M. D. Elwardany, F. Y. Rad, S. Underwood, M. J. Farrar, and R. R. Glaser. *Long-Term Aging of Asphalt Mixtures for Performance Testing and Prediction*. NCHRP 09-54. North Carolina State University, 2013.
  18. Ling, M., X. Luo, F. Gu, and R. L. Lytton. Time-Temperature-Ageing Depth Shift Functions for Dynamic Dulus Master Curves of Asphalt Mixture. *Construction and Building Materials*, Vol. 157, 2017, pp. 943–951.
  19. Rasool, R., H. Yao, A. Hassan, S. Wang, and H. Zhang. In-Field Ageing Process of High Content SBS Modified Asphalt in Porous Pavement. *Polymer Degradation and Stability*, Vol. 155, 2018, pp. 220–229.
  20. Ahmed, E. I., S. A. M. Hersp, S. K. P. Samy, S. D. Rubab, , and G. Warburton. Effect of Warm Mix Additives and Dispersants on asphalt rheological, ageing and failure properties. *Construction of Building Materials*, Vol. 37, 2012, pp. 493–498.
  21. Zhang, H., X. Fu, H. Jiang, X. Liu, and L. Lv. The Relationship between Asphalt Ageing in Lab and Field Based on the Neural Network. *Road Materials and Pavement Design*, Vol. 16, No. 2, 2015, pp. 493–504.
  22. Lu, X., and U. Isacsson. Effect of Ageing on Bitumen Chemistry and Rheology. *Construction and Building Materials*, Vol. 16, 2002, pp. 15–22.
  23. Wang, P. E. Y., Y. Wen, K. Zhao, D. Chong, and A. S. T. Wong. Evolution and Locational Variation of Asphalt Binder Ageing in Long-Life Hot-Mix Asphalt Pavements. *Construction and Building Materials*, Vol. 68, 2014, pp. 172–182.
  24. Shalaby, A. Modelling Short-Term Ageing of Asphalt Binders Using the Rolling Thin Film Oven Test. *Canadian Journal of Civil Engineering*, Vol. 29, 2002, pp. 134–145.
  25. Grilli, A., M. Bocci, F. Crdone, C. Conti, and E. Giorgini. Laboratory and In-Plant Validation of Hot Mix Recycling Using a Rejuvenator. *International Journal of Pavement Research and Technology*, Vol. 6, No. 4, 2013, pp. 364–671.
  26. Jing, R., A. Varveri, X. Liu, A. Scarpas, and S. Erkens. Laboratory and Field Ageing Effect on Bitumen Chemistry and Rheology in Porous Asphalt Mixture. *Transportation Research Record: Journal of the Transportation Research Board*, 2019. 2673(3): 365–374.
  27. van Lent, D., S. Mookhoek, D. van Vliet, C. Giezen, and G. Leegwater. Comparing field ageing to artificial laboratory ageing of bituminous binders for porous asphalt concrete using black space graph analysis. In *Proc., 6th Euraspphalt and Eurobitumn Congress*, Prague, Czech Republic, 1–3 June 2016.
  28. Newcomb, D., A. E. Martin, F. Yin, E. Arambula, E. S. Park, A. Chowdhury, R. Brown, C. Rodezno, N. Tran, E. Coleri, D. Jones, J. T. Harvey, and J. M. Signore. *Short-term Laboratory Conditioning of Asphalt Mixtures*. Report NCHRP 815. Transportation Research Board, Washington, D.C., 2015.
  29. Bell, C. A., and D. Sosnovske. *Aging: Binder Validation*. Strategic Research Program Report no. SHRP-A-384. National Research Council, Washington, D.C., 1994.

30. Van den Bergh, W. *The Effect of Aging on Fatigue and Healing Properties of Bituminous Mortars*. PhD thesis, Delft University of Technology, Delft University, 2011.
31. Brown, S. F., and T. V. Scholz. Development of Laboratory Protocols for the Aging of Asphalt Mixtures. *Proc., 2nd Eurasphalt and Eurobitume Congress*, Vol. 1, 2000, pp. 83–90.
32. Mollenhauer, K., and V. Mouillet. *Re-Road: End of Life Strategies of Asphalt Pavements*. European Commission DG Research, Ixelles, Belgium, 2011.
33. Harrigan, E. T. *Research Results Digest 324-Simulating the Effects of Hot Mix Asphalt Aging for Performance Testing and Pavement Structural Design*. National Cooperative Highway Research Program, 2007.
34. West, R. C., D. E. Watson, P. A. Turner, and J. R. Casola. *Mixing and Compaction Temperatures of Asphalt Binders in Hot-Mix Asphalt*. No. Project 9-39. National Cooperative Highway Research Program, 2010.
35. Reed, J. *Evaluation of the Effects of Aging on Asphalt Rubber Pavements*. Masters thesis. Arizona State University, 2010.
36. Betti, G., G. Airey, K. Jenkins, A. Marradi, and G. Tebaldi. Active Filler's Effect on Insitu Performances of Foam Bitumen. *Road Materials and Pavement Design*, Vol. 18, No. 2, 2017, pp. 281–296.
37. Hagos, E. T., A. A. A. Molenaar, and M. F. C. van de Ven. Chemical Characterization of Laboratory and Field Bitumen Ageing in Porous Asphalt Concrete. *Advanced Testing and Characterization of Bituminous Materials*, 2009, pp. 173–184.
38. Khedoe, R. N., A. A. A. Molenaar, and M. F. C. van de Ven. Low Temperature Behavior of Very Hard Bituminous Binder Materials for Road Applications. *Proc. 6th RELEM Conference on Cracking in Pavement*, 2008, pp. 481–490.
39. Jing, R., A. Varveri, X. Liu, A. Scarpas, and S. Erkens. Ageing Effect on Chemo-Mechanics of Bitumen. *Road Materials and Pavement Design*, Vol. 22, No. 5, 2019, pp. 1044–1059.
40. Jing, R., A. Varveri, X. Liu, A. Scarpas, and S. Erkens. Study on the Asphalt Pavement Response in the Accelerated Pavement Testing Facility. *Proc., 9th International Conference on Maintenance and Rehabilitation of Pavements*. 2020, pp. 871–880.
41. Varveri, A., S. Avgerinopoulos, C. Kasbergen, A. Scarpas, and A. Collop. Influence of Air Void Content on Moisture Damage Susceptibility of Asphalt Mixtures: Computational Study. *Transportation Research Record: Journal of the Transportation Research Board*, 2015. 2446(3): 8–16.
42. Jing, R., A. Varveri, D. van Lent, and S. Erkens. Laboratory and Field Ageing of Asphalt Mixtures. *Advances in Materials and Pavement Performance Prediction*, San Antonio, TX, US, 2020.
43. Lamontagne, J., P. Dumas, V. Mouillet, and J. Kister. Comparison by Fourier transform Infrared (FTIR) Spectroscopy of Different Ageing Techniques: Application to Road Bitumens. *Fuel*, Vol. 80, No. 4, 2001, pp. 483–488.
44. Green, J. B., S. K. T. Yu, C. D. Pearson, and J. Reynolds. Analysis of Sulfur Compound Types in Asphalt. *Energy Fuels*, Vol. 7, No. 1, 1993, pp. 119–126.
45. Menapace, I., W. Yuming, and E. A. Masad. Effects of Environmental Factors on the Chemical Composition of Asphalt Binders. *Energy Fuels*, Vol. 33, No. 4, 2018, pp. 2614–2624.
46. Menapace, I., W. Yiming, and E. A. Masad. Investigation of Moisture Damage Coupled with Ageing of Asphalt Binder. *Proc., International Conference on Advances in Materials and Pavement Performance Prediction*, 2018, pp. 431–434.
47. Jing, R., A. Varveri, X. Liu, A. Scarpas, and S. Erkens. Rheological, Fatigue and Relaxation Properties of Aged Bitumen. *International Journal of Pavement Engineering*, Vol. 21, No. 8, 2020, pp. 1024–1033.
48. Bahia, H., H. Zhai, K. Bonnetti, and S. Kose. Non-Linear Viscoelastic and Fatigue Properties of Asphalt Binders. *Journal of the Association of Asphalt Paving Technologists*, Vol. 68, 1999, pp. 1–34.
49. Bahia, H., H. Zhai, M. Zeng, Y. Hu, and P. Turner. Development of Binder Specification Parameters Based on Characterization of Damage Behaviour. *Journal of the Association of Asphalt Paving Technologists*, Vol. 70, 2002, pp. 442–470.
50. Jafari, M., and A. Babazaseh. Evaluation of Polyphosphoric Acid-Modified Binders Using Multiple Stress Creep and Recovery and Linear Amplitude Sweep Tests. *Road Materials and Pavement Design*, Vol. 17, No. 4, 2016, pp. 859–876.
51. Pasetto, M., G. Giacomello, E. Pasquini, and I. Antunes. Laboratory Evaluation of the Flexural Properties of Membrane-Reinforced Asphalt System. *Proc., World Conference on Pavement and Asset Management*, 2019, pp. 277–283.
52. Wang, Z., L. Cai, X. Wang, C. Xu, B. Yang, and J. Xiao. Fatigue Performance of Different Thickness Structure Combinations of Hot Mix Asphalt and Cement Emulsified Asphalt Mixtures. *Materials*, Vol. 11, No. 7, 2019, p. 1145.